Research Article

Influence of interval type-2 fuzzy control approach for a grid-interconnected doubly-fed induction generator driven by wind energy turbines in variable-speed system

I. Hamdan[1] · **Marwa M. M. Youssef**[1] · **Omar Noureldeen**[1,2]

Abstract

This paper suggests a developed control technique using an interval type-2 fuzzy logic control (FLC) tuned PI for optimum torque adjustment for wind turbines operated by doubly fed induction generator (DFIG). The suggested control regulates the error of the mechanical rotor speed to enhance the performance of the torque and the output power results in the study system's overall performance improving. The suggested control combines the advantages of the two techniques: fast response of conventional PI control and adaptively properties of interval type-2 FLC. The studied system is a wind farm of 9 MW composed of 6 wind turbines of 1.5 MW each. Wind speed functions of several types are studied such as step change, extreme change, and constant high speed. The results indicate how the power and optimal torque have fast response with interval type-2 FLC tuned PI compared to the type-1 fuzzy tuned PI and conventional PI control. The simulated results deduce that the suggested interval type-2 FLC can enhance the wind energy system's stability and reliability in a better manner compared to the type-1 FLC and conventional PI.

Article Highlights

- This work has demonstrated the efficacy of an interval type-2 FLC adjusted PI in regulating wind turbine rotor speed.
- The suggested control combined the rapid performance of the PI approach and intelligent control adaptive characteristics.
- The performance of optimum torque and output power is better with fuzzy type-2 than its type-1 and conventional control.

Keywords Fuzzy logic control · Bidirectional converter · Doubly-fed induction generator · Wind turbine · Type-2 fuzzy logic

1 Introduction

In the last three decades, the renewable-energy sources have garnered a lot of interest worldwide. Undoubtedly, one of the renewable energy sources with the highest global growth is wind energy, that's because it has qualities like being widely available, pure, and completely renewable [1, 2]. The doubly-fed induction generator (DFIG), because of its unique properties of low power electronic converter size (about 25% to 30% of nominal

✉ I. Hamdan, IbrahimHamdan86@eng.svu.edu.eg | [1]Electrical Engineering Department, Faculty of Engineering, South Valley University, Qena 83523, Egypt. [2]Electrical Engineering Department, Faculty of Engineering, Al Baha University, Al Aqiq 65779-7738, Saudi Arabia.

power), good efficiency, and broad range of speed control, becomes one of the most electric approaches employed with wind turbine (WT) [3] so it is reliable for variable-speed WT (VSWT) system technique. DFIG has a different and distinctive network connection as the stator is connected to the system and the same connection is for the rotor. This subsequently enables full control over the active and reactive power exchange. To obtain the highest value of power at any wind speed, VSWT uses two control methods for regulating speed, they are indirect-speed control (ISC) and direct-speed control (DSC). Every time there is a change in wind speed, the DSC modifies the ideal turbine rotor speed and controls it to obtain the optimal amount of torque whereas ISC uses the dynamic-stable properties of VSWT to calculate the reference torque associated with the highest value in the power curve for each WT rotor speed [4]. The fields of optimal torque production and speed control include a lot of published material. Classic controllers like PI, PD, and PID control are employed in earlier studies for their simplicity. However, these typical controllers are unreliable for nonlinear complex systems because they only operate properly within a limited working range, and they are enormously sensitive to changes in system parameters. Sliding mode control techniques, passivity-based controllers, linear averaged controllers, feedback linearizing controllers, and other nonlinear controllers have all been presented. The complexity of the system, the difficulty of making precise assertions, and the difficulty of making broad generalizations about its behavior pose the biggest obstacles for these methodologies [5].

On the other hand, to tackle the robust control of ambiguous, complicated, and dynamic systems, artificial intelligence approaches including fuzzy logic control (FLC) are now widely employed as the significant advantage of these controllers is that they need no knowledge of the mathematical design model or be familiar with the system problems. The interval type-2 adaptive fuzzy approach, which is an expanded form of type-1 fuzzy logic, is created to represent a variety of dynamic uncertainties and non-linearity that arise in tracking errors.

Previous studies in the topic of speed regulators provide many sorts of controllers, in [6], To create reference torque, the maximum power tracking method is used to modify an ideal rotor speed reference based on PI controller. In order to regulate the speed of induction generators, the research in [7] examines the performance of two predictive control systems, one of these controllers uses a finite control set-model approach, and the other uses a continuous control set-model strategy combined with space vector-pulse width modulation. In [8], the fuzzy technique with inputs of rotor speed and wind speed is used to suggest a speed controller for WT based on DFIG, and the algorithm that utilized

to tune the controller settings is the particle swarm optimization (PSO). The study in [9] presents a reliable control method for the optimal torque determination for the WT based on the super-twisting technology (STW) that tracks maximum power, which is preferred over the conventional sliding mode algorithm, the results are compared with PI controller to deduce the efficacy of the proposed control on improving the dynamic system performance. In [1], STW sliding mode controller with fractional order calculation is proposed to regulate speed to generate reference torque and the results of this robust, non-linear control are compared with PI control. The authors, in [10], provide a neural network controller for speed adjustment with straightforward connection weight modification taking system parameter resilience into account. The fuzzy PI approach is implemented in [11] for speed regulation and the scheme results are with those of conventional PI control. A novel DSC prediction method using the double-cost function that has an adjusted duty ratio is presented in [12] to control permanent-magnet synchronous machine. Authors in [13] present a fuzzy PI approach for speed control with a new switching function in a permanent-magnet synchronous machine to generate reference q-axis current corresponding to optimum torque. The optimum torque is adjusted in [14] by regulating the rotor speed which is estimated using a model reference adaptive system.

There are previous studies that implemented interval type-2 FLC to control VSWT as in [15], the authors applied the interval type-2 FLC to control the rotor voltage of the DFIG to enhance active and reactive power performance. In [16], the authors applied the interval type-2 FLC in rotor current regulation to enhance active and reactive power performance. In [17], the authors also applied the interval type-2 FLC to control the rotor voltage of the DFIG to enhance active and reactive power performance. In [18], the authors used interval type-2 FLC power system stabilizer (PSS) to decrease uncertainties and increase the power system dynamic stability margin. In [19], the authors applied interval type-2 FLC for rotor voltage control. In [20], the authors applied interval type-2 FLC with maximum power point algorithm, the controlling technique is developed through the nonlinear systems. In [21], the authors applied interval type-2 FLC using the fractional sliding mode approach to substitute the sliding discontinuous signals. The control scheme is achieved from the stability study of Lyapunov's approach. In [22], the authors applied interval type-2 FLC to regulate the rotor and stator currents to control the rotor and stator voltages.

In contrast to the previous research, this paper suggests an adaptive interval type-2 FLC tuned PI

controller to regulate rotor speed to enhance the performance of the torque and the output power causes the system under study to be improved overall. The interval type-2 FLC adaptive PI controller is a combination of conventional PI control that regulates the rotor speed and the intelligent control that is used for adjusting the PI settings in according to the state of the system, this hybrid control has the advantages of both techniques: rapid performance of the PI approach and the interval type-2 FLC's adaptive characteristics. The main objectives of this study are adjusting the optimum torque and improving the performance of power, torque, and current using type-2 FLC tuned PI compared to other control methods (conventional PI, type-1 FLC PI).

This paper has the following structure: Introduction is presented in Sect. 1. Section 2 illustrates wind energy system modeling and configuration. Sections 3 and 4 present overviews of fuzzy logic configuration of type-1 and interval type-2 respectively. Section 5 shows the proposed design of interval adaptive type-2 fuzzy PI control. The model configuration studied in this paper and the simulated results are shown in Sect. 6. The final conclusion is set out in Sect. 7.

2 Wind energy conversion system configuration and model

The DFIG-based variable speed WT (VSWT) architecture includes a unique electrical arrangement. A gearbox links the generator with the WT's rotor and the stator-winding of the generator is linked directly to the electric network whereas the rotor-winding is connected by two converters which are called back-to-back converters that comprise of grid-side converter (GSC) and rotor-side converter (RSC). Constant DC bus voltage is attained using GSC control whereas the RSC's function is to modify the generator's torque and control the reactive power transferred to the grid through the stator. Figure 1 provides an illustration of the DFIG-based WT's electric setup.

2.1 Wind turbine model

The following equation describes how wind speed (v_w) relates to the recovered power by the turbine extracted from kinetic energy of the wind (P_m) [23]:

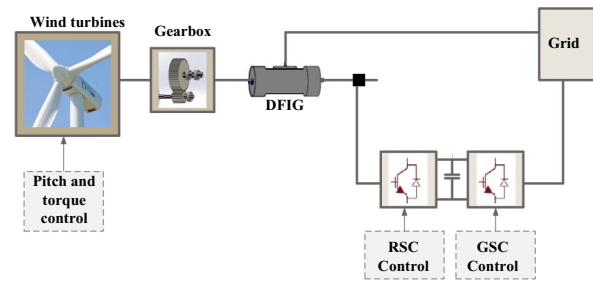$$P_m = 0.5 \rho \pi R^2 V_w^3 C_p \tag{1}$$

Fig. 1 DFIG electric arrangement

where R is length of the WT blade and C_p is the power coefficient as indicated by of the tip speed ratio λ, given by:

$$\lambda = \frac{R\Omega_t}{V_w} \tag{2}$$

where Ω_t is the angular turbine rotor speed. The maximum value of C_p theoretically equals 0.593. The turbine rotor torque is expressed by dividing the recovered power by the rotation speed of the turbine as follows [23]:

$$T_t = \frac{P_m}{\Omega_t} = \frac{\rho \pi R^3 V_w^2}{2\lambda} C_p \tag{3}$$

The rotor blades are controlled by the pitch control which checks the recovered power by the WT and turns the rotor blades in such a way to make the rotor blades be optimally angled and optimize power generation at all wind speeds.

2.2 Shaft system model

The two-mass model having soft linkage between the two inertia parts represented by the damping and stiffness coefficients (D_{tm} and K_{tm}) can be used to represent the drive train. The masses inertia on the turbine side is J_t whereas J_m is the generator side masses inertia. As follows is an expression for the dynamic equations [4]:

$$J_t \frac{d\Omega_{t\_ar}}{dt} = T_{t\_ar} - D_t\Omega_{t\_ar} - T_{em} \tag{4}$$

$$J_m \frac{d\Omega_m}{dt} = T_{em} - D_m\Omega_m + T_{em} \tag{5}$$

$$\frac{dT_{em}}{dt} = K_{tm}(\Omega_{t\_ar} - \Omega_m) + D_{tm}\left(\frac{d\Omega_{t\_ar}}{dt} - \frac{d\Omega_m}{dt}\right) \tag{6}$$

where the turbine driving torque and rotational speed are indicated in the fast shaft by the variables T_{t_ar}, Ω_{t_ar}.

The specifications for the WT and machine's friction coefficients are D_t and D_m. T_{em} is the generator driving torque.

2.3 Generator model

Voltage and flux equations are rebuilt in direct and quadrature (d-q) rotating frames as follows to provide the DFIG mathematical dynamic model [6, 24]:

$$V_{sd} = R_s i_{sd} + \frac{d\varphi_{sd}}{dt} - \omega_s \varphi_{sq} \qquad (7)$$

$$V_{sq} = R_s i_{sq} + \frac{d\varphi_{sq}}{dt} + \omega_s \varphi_{sd} \qquad (8)$$

$$V_{rd} = R_r i_{rd} + \frac{d\varphi_{rd}}{dt} - \omega_r \varphi_{rq} \qquad (9)$$

$$V_{rq} = R_r i_{rq} + \frac{d\varphi_{rq}}{dt} + \omega_r \varphi_{rd} \qquad (10)$$

$$\varphi_{sd} = L_s i_{sd} + L_m i_{rd} \qquad (11)$$

$$\varphi_{sq} = L_s i_{sq} + L_m i_{rq} \qquad (12)$$

$$\varphi_{rd} = L_r i_{rd} + L_m i_{sd} \qquad (13)$$

$$\varphi_{rq} = L_r i_{rq} + L_m i_{sq} \qquad (14)$$

where φ, I, V, and L are magnetic fluxes, current, voltage, and inductance. While r and s subscript relate to rotor and stator, the mutual inductance is symbolized by L_m. ω_s and ω_r are voltage angular frequency of the stator windings and the rotor winding respectively. The torque (T_{em}) formula. is as denoted by the following equation [4]:

$$T_{em} = \frac{3}{2} P \frac{L_m}{L_s}(\varphi_{qs} i_{dr} - \varphi_{ds} i_{qr}) \qquad (15)$$

where P is the number of pole pairs. When the wind speed is between the maximum and lowest speed limits, the wind turbine operates at a variable speed, with the turbine control tracking the maximum power curve to adjust the ultimate power at each wind speed. The terms DSC and ISC refer to two separate categories of speed controllers. By establishing the ideal speed that corresponds to the highest power and then altering the optimum torque, DSC can monitor the maximum power curve more precisely with quicker dynamics as shown in Fig. 2.
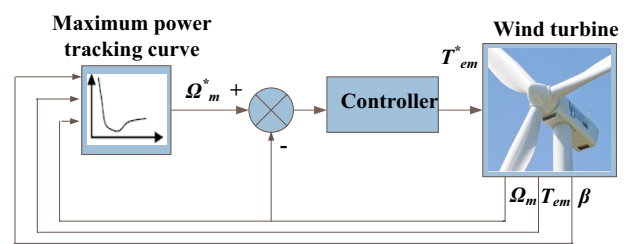

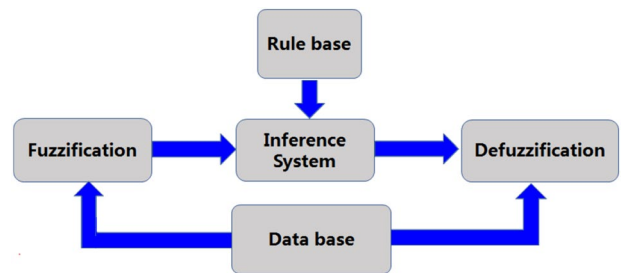**Fig. 2** Control scheme for optimum torque

Fig. 3 Type-1 fuzzy control configuration

3 Overview of type-1 fuzzy logic sets

Based on the system operator's knowledge, the FLCs are regarded as non-linear intelligent controllers that are self-adjusting and have very extreme accuracy and reliability. Instead of using sharp or numerical variables, FLC instead employs linguistic variables that allow any variable with a value between 0 and 1 to have a state, unlike Boolean logic that allows states 0 or 1. As the system measurements are nonfuzzy, so these must be converted to crisp values. The four main stages of the primary closed-loop fuzzy control setup shown in Fig. 3 are: fuzzification process, set of fuzzy rules, decision-making logic, defuzzification. The process of transforming crisp variables into linguistic variables is called fuzzification. The fuzzy control operation is inferred by decision-making logic from awareness of specifications of linguistic variable and the control set of rules. Defuzzification is required to transform the fuzzy control sets produced by the fuzzy algorithm into numerical variables.

A membership function (MF) symbolized as $\mu_A(x)$ with elements in the domain [0, 1] express the type-1 fuzzy set (FS) in the universe X. The following is the definition of an element's membership degree in the set:

$$A = (x, \mu_A(x)) \forall x \in X, \mu_A : X \to [0, 1] \qquad (16)$$

where $\mu_A(x)$ represents the membership degree of the element $x \in X$ to the set A. The centre of gravity, maximum membership principle, mean-max membership, centre

of sums, or weighted average approach can be used to execute the defuzzification procedure [5].

The Mamdani-Larsen FS, the Takagi–Sugeno–Kang (TSK) FS, the generalized FS (GFS), and others are examples of typical FS models, with TSK FSs being the most researched models thanks to their great efficacy. A major range of dynamic non-linear control issues may be solved using FLC based on the TSK approach, which has more and preferable solutions [25, 26]. The MFs produced by the Sugeno are linear or constant.

The TSK FS is a conventional FS system characterized by its excellent nonlinear modelling capabilities, has human-like interpretation skills, and is very adaptable. This is how TSK FS, which uses the kth fuzzy rule as its rule base, is represented [27]:

$$IF\ x_1\ is A_1^k\ and\ x_2\ is\ A_2^k.....and\ x_d\ is A_d^k$$
$$THEN\ y^k = f^k(x) = p_0^k + p_1^k x_1 + ... + p_d^k x_d, k = 1, .., K \tag{17}$$

where, A_i^k $(1 < i < d)$ is a FS, the fuzzy rules number is denoted by K, The rule consequents' parameter is defined by P_n^K $(n = 0, 1 ..., d)$, the number of features is d, the index of fuzzy rules is k, and y^k is the fuzzy output. The output of the TSK FS $f(x)$ with defuzzification process using the center of gravity method can be expressed as follows [25]:

$$f(x) = \sum_{k=1}^{K} \frac{u^k(x)}{\sum\limits_{k=1}^{K} u^k(x)} f^k(x) = \sum_{k=1}^{K} \tilde{u}^k(x) f^k(x) \tag{18}$$

where $u^k(x)$ and $\tilde{u}^k(x)$ define the fuzzy MF and the normalized fuzzy membership related to FS, respectively.

4 Basic concept of interval type-2 fuzzy logic sets

Karnik and Mendel have presented the interval type-2 fuzzy logic system (FLS) in [28], An interval type-2 FS is one in which membership values are type-1 FSs on the range [0,1]. One fuzziness depends on another fuzziness in interval type-2 FS, this dependency makes the interval type-2 FS a complex subject that simulates the uncertainty better than conventional FLSs. The product space of the primary and secondary variables contains fuzzy relationships for both the type-1 FSs and the inter0076al type-2 FS [29]. Contrastingly, these variables are independent in type-1 FS, but the secondary variable in interval type-2 FS is inherently reliant on the primary variable. For high levels of uncertainties, interval type-2 FLC is more reliable compared to type-1 FLC this is because that type-1 FS deals with the unknowns related to the FLS inputs and outputs by employing crisp MFs that have already been chosen, the reality that the real
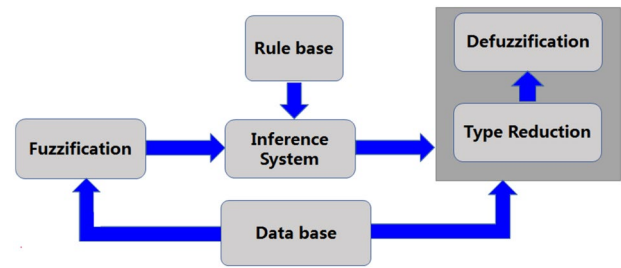

Fig. 4 Interval type-2 FLS configuration

membership degree is unknown, has ceased to exist. Interval type-2 FS, in contrast to type-1 FS, is defined by a fuzzy MF whose values are all FS in the range of [0,1]. So, the nature of the MFs is the sole distinction between interval type-2 FLC and type-1 FLC. The MFs of interval type-2 FS are 3-dimension and have a footprint of uncertainty (FOU) [30]. Thus, interval type-2 FS is more appropriate to deal with the linguistic and numerical ambiguities and improves the performance of the system for particular applications.

An interval type-2 FLS comprised of two MFs (primary and secondary). An interval type-2 FLC's primary membership degree is a regular FS in [0, 1], however, the secondary membership is a specific number in [0, 1] range. Following the fuzzification process, fuzzy inference, interval type-reduction, and defuzzification, the crisp output of interval type-2 FLS is obtained. Interval type-2 MFs are used to transform crisp inputs to fuzzy inputs during the fuzzification process. The interval type-2 FS output is converted to type-1 FS in an extra stage known as type reduction, which is then applied to the defuzzification process to provide a crisp output. Algorithms for type reduction can be used in a variety of ways, including height, centroid, center-of-set, and modified height [16]. The configuration of interval type-2 FLS is shown in Fig. 4 [15].

A description of an interval type-2 FS (labeled $\tilde{A}$) would be [31, 32]:

$$\tilde{A} = \{((x, u), \mu_{\tilde{A}}(x, u)) \forall x \in X, \forall u \in J_x \subseteq [0, 1]\} \tag{19}$$

where $x \in X$, and $u \in J_x \subseteq [0, 1]$ are the primary and secondary variables, respectively with an interval type-2 MF $\mu_{\tilde{A}}(x, u)$ where $0 \leq \mu_{\tilde{A}}(x, u) \leq 1$. J_x is called the primary membership of a type-2 FS of x. Alternative type-2 FSs were proposed to reduce the computational complexity of universal interval type-2 FLSs. The following is a description of an interval type-2 set $\tilde{A}$ [31]:

$$\tilde{A} = \int_{x \in X} \int_{u \in J_x} 1/(x, u), J_x \subseteq [0, 1] \tag{20}$$

$\widetilde{A}: X \rightarrow \{[a, b]: 0 \le a \le b \le 1\}$. The grey area of Fig. 5 represents the FOU of $\widetilde{A}$, which is the aggregate of all the primary memberships and represents the degree of uncertainty around $\widetilde{A}$ [33].i.e.:

$$FOU(\tilde{A}) = \cup_{\forall x \in X} J_x = \{(x, u) : u \in J_x \subseteq [0, 1]\} \qquad (21)$$

Two type-1 MFs, denoted by the letters $\underline{\mu}_{\widetilde{A}}(x)$ and $\overline{\mu}_{\widetilde{A}}(x)$, surround the FOU ($\widetilde{A}$). These MFs are known as the lower MF and upper MF respectively [33].

$$\overline{\mu}_{\widetilde{A}}(x) = FO\overline{U}(\widetilde{A}), \forall x \in X \qquad (22)$$

$$\underline{\mu}_{\widetilde{A}}(x) = FO\underline{U}(\widetilde{A}), \forall x \in X \qquad (23)$$

whereas J_x is given by the following formula [32]:

$$J_x = \{(x, u) : u \in [\overline{\mu}_{\widetilde{A}}(x), \underline{\mu}_{\widetilde{A}}(x)]\} \qquad (24)$$

An embedded FS $\widetilde{A}_e$ for a continuous universe of discourse X and μ is defined as follows [17]:

$$\widetilde{A}_e = \int_{x \in X} [1/u]/x, u \in J_x \qquad (25)$$

The set $\widetilde{A}_e$ is inserted in A so that the secondary MF is one for every value of x. Many different type-1 FSs are embedded to create the interval type-2 FS where each type-1 FS is combined to generate the FOU.

Type-2 FSs have the advantage of being able to handle with higher modelling and uncertainty levels found in real-world applications, particularly control systems. Additionally, a fuzzy MF with values that are all FS in the range [0,1] defines the interval type-2 FS, in contrast to type-1 FS. Therefore, the only difference between interval type-2 FLC and type-1 FLC is the nature of the MFs. Interval type-2 FS MFs are three-dimensional and feature an uncertainty footprint. The shortcomings of this control, however, are its inability to recognize artificial intelligence (AI) as neural system-type designs and its inconsistently precise
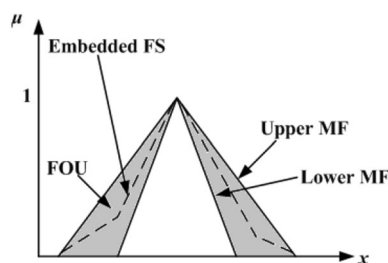

Fig. 5 Triangular interval type-2 FS $\widetilde{A}$

fuzzy reasoning. Therefore, the results are seen based on assumptions and could not be widely accepted.

5 Proposed design of interval type-2 fuzzy speed control

The speed control loop that establishes the reference torque is the primary component of the conventional control scheme of the direct speed control technique as illustrated in Fig. 6a, and this regulated control is done via a PI controller. The control responsible for the maximum power point tracking (MPPT) in this research uses the tracking curve method that determines the reference speed. By comparing the reference speed value to the actual observed speed value, the error signal is adjusted. The PI controller then receives the speed error as an input. The maximum power curve, which gives the optimal torque corresponding to the maximum output power from the WT for each wind speed, determines the reference speed by following the route of maximum value of power [34].

In order to enhance system stability during the disturbance, the interval type-2 FLC adaptive PI is suggested as an alternative for the PI speed controller. In order to get a preferred reaction in the dynamic and stable circumstances of the system, interval type-2 FLC adaptive PI combines an interval type-2 fuzzy technique that is adaptable with a conventional PI controller that reacts rapidly. The fuzzy technique is in charge of adjusting the PI controller's parameter based on the state of the system. Therefore, interval type-2 FLC adaptive PI control combines the benefits of conventional PI technology with intelligent control, which in turn enhances the PI controller's performance and the system stability is further improved.

In this study, interval type-2 FLC adaptive PI is used to simulate the DFIG-based WT system model and is compared to type-1 FLC adaptive PI in order to determine which is more successful in addressing system uncertainty. Figure 6b, c depict the recommended control approach using type-1 and type-2 FLC.

In this paper, the fuzzy controller of type-1 and type-2 are with two input-signals and one output-signal. The error signals and the derivative of the error are the inputs and fuzzified using three triangular MFs. The FSs are classified as Negative (N), Zero (Z), Positive (P). Figures 7 and 8 display the planned MFs of error for type-1 and type-2 FLCs, respectively, and the same MFs are for the derivative of the error. The universe of discourse's upper and lower limits for all inputs and outputs are set at + 1 to 1. The output is the change in the PI parameter, and the designed FSs of the output are Positive-Small (PS), Positive-Large (PL), Zero (Z), Negative-Small (NS), and Negative-Large (NL). The error

Fig. 6 Control strategy of speed regulator. **a** conventional PI, **b** interval type-1 FLC tuned PI, **c** interval type-2 FLC tuned PI
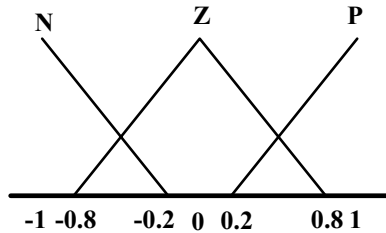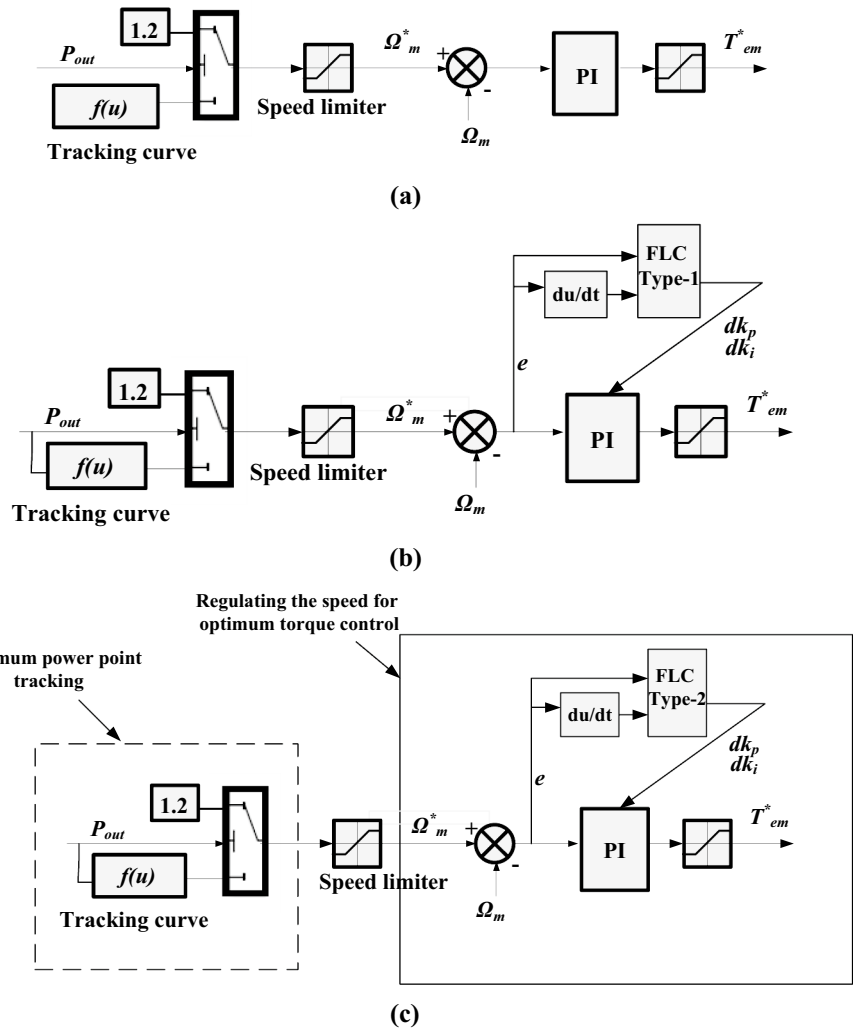

(a)

(b)

(c)

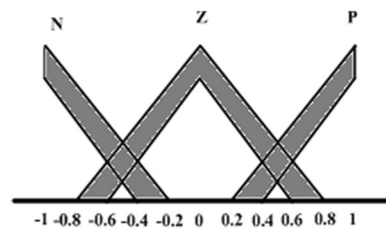**Fig. 7** MFs of the speed error for type-1 fuzzy

Fig. 8 MFs of the speed error for interval type-2 fuzzy

(e) of rotor speed (Ω_m) signal and the change of the error signals (Δe) derived as follows:

$$e = \Omega_{mref} - \Omega_m \tag{26}$$

$$\Delta e = e(k) - e(k-1) \tag{27}$$

where Ω_{mref} is the reference rotor speed, $e(k)$ is the current speed error, and $e(k-1)$ is the previous speed error.

The fuzzy logic controller is implemented using a Sugeno-type fuzzy inference system, and the fuzzy rules are designed as displayed in Table 1. The expressions describing the change in PI parameters are given by [35]:

$$K_p(k+1) = K_p(k)[1 \pm dk_p] \tag{28}$$

$$K_i(k+1) = K_i(k)[1 \pm dk_i] \tag{29}$$

where dk_p and dk_i are the output of the fuzzy approach, K_p and K_i are the PI controller's settings. The symbols k and $k+1$ refer to the current and the next parameters.

Table 1 Fuzzy rules

dk_p, dk_i		e		
		N	Z	P
Δe	N	NL	NS	Z
	Z	NS	Z	PS
	p	Z	PS	PL

6 Model configuration and simulated results

The model under study in this paper consists of six 1.5 MW WTs each with 4.32 inertia constant linked to the utility grid through a step-up transformer, a transmission line measuring 10 km in length, and a step-down transformer, as illustrated in Fig. 9. The studied cases are three different wind speed functions: step change, extreme change, and constant wind speed with a high value that equals 18 m/sec. In each case, output active power with interval type-2 FLC tuned PI control is studied with comparison to type-1 FLC PI control and conventional PI control.
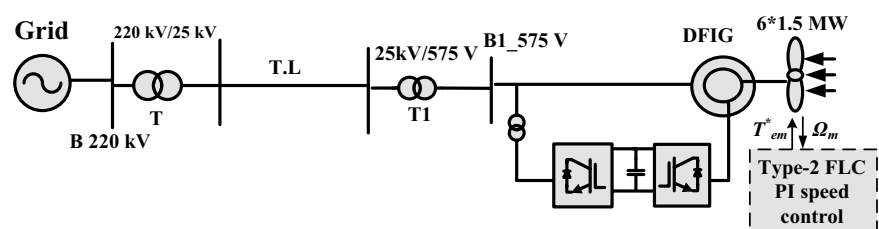
6.1 Step change wind speed

In this case, the step-change wind speed is changed from 15 m/sec to 12 m/sec occurred at 7 s as depicted in Fig. 10a. The performance of the suggested method is compared with type-1 FLC tuned PI and conventional PI control. The reference signals for torque and active power are set at 0.75 pu and 9 MW respectively at 15 m/sec and set at 0.6 pu and 8.2 MW respectively at 12 m/sec. The reference torque reaches the steady-state value at 2 s for 15 m/sec wind speed and at 15.3 s for 12 m/sec with interval type-2 FLC tuned PI controller. Compared to other control methods, the interval type-2 FLC tuned PI system approaches to the reference value more adequately, as the overshoot and undershoot are much smaller in it as shown in Fig. 10b. The obtained active power is depicted in Fig. 10c with speed regulator using interval type-2 FLC tuned PI controller and compared with using type-1 FLC tuned PI control and conventional PI control. At the beginning with a speed of 15 m/sec, the power reaches the steady-state value that equals 9 MW at 2 s with interval

type-2 FLC with no overshoot approximately, however with type-1 FLC and with conventional controller reaches 9 MW at 3.7 s and 4.7 s, respectively with peak overshoot equals 9.78 and 9.98 MW respectively. When the wind changes to 12 m/sec, the power reaches the steady-state value that equals 8.2 MW at 10 s with interval type-2 FLC more smoothly than other controllers. However, the power reaches the steady-state value at 12.8 s with type-1 FLC and at 18 s with conventional controller. Figure 10d illustartes the results of the RMS output current, it is also faster and smoother with interval type-2 FLC tuned PI controller compared to other ones and the overshoot is much smaller in it. The overshoot of the output current for 15 m/sec wind speed equlas 0.65 pu for type-2 FLC however it equals 0.68 and 0.7 pu for type-1 FLC tuned PI and conventional PI respectively. There is no overshoot of the output current for 12 m/sec wind speed with type-2 and type-1 FLC tuned PI however it equals 0.43 pu for conventional PI.

6.2 Extreme change wind speed

In this case, the wind speed changes extremely between 15 m/sec, 12.4 m/sec, and 22 m/sec as shown in Fig. 11a. The reference torque reaches the steady-state that equals (0.75 pu) at the beginning of the extreme wind speed faster and smoother with interval type-2 fuzzy tuned PI compared to other controllers with a little overshoot equals 0.76 pu. However, the overshoot equals 0.8 pu and 0.82 pu with type-1 FLC tuned PI and conventional PI, respectively. With the PI controller, the torque is about to cross the limited value, so it is limited to 1 pu at wind speed of 22 m/sec as depicted in Fig. 11b. When the wind speed returned to 15 m/sec, the reference torque reaches the steady-state with interval type-2 FLC at 13 s, however, it reaches this value at 14.2 s and 17 s with type-1 FLC and conventional PI, respectively. In the beginning with a speed of 15 m/sec, the power with interval type-2 FLC has no overshoot approximately. However, the peak overshoot with type-1 FLC equals 9.78 and with conventional PI it equals 9.98 MW. When the wind speed changes from 12.4 to 22 to 12.4 m/sec, the power changes more smoothly with FLC interval type-2 PI than other controllers. When the wind speed returns to 15 m/sec, the time when the active power reaches steady-state value with interval type-2 FLC tuned PI equals 12.3 s. However, it

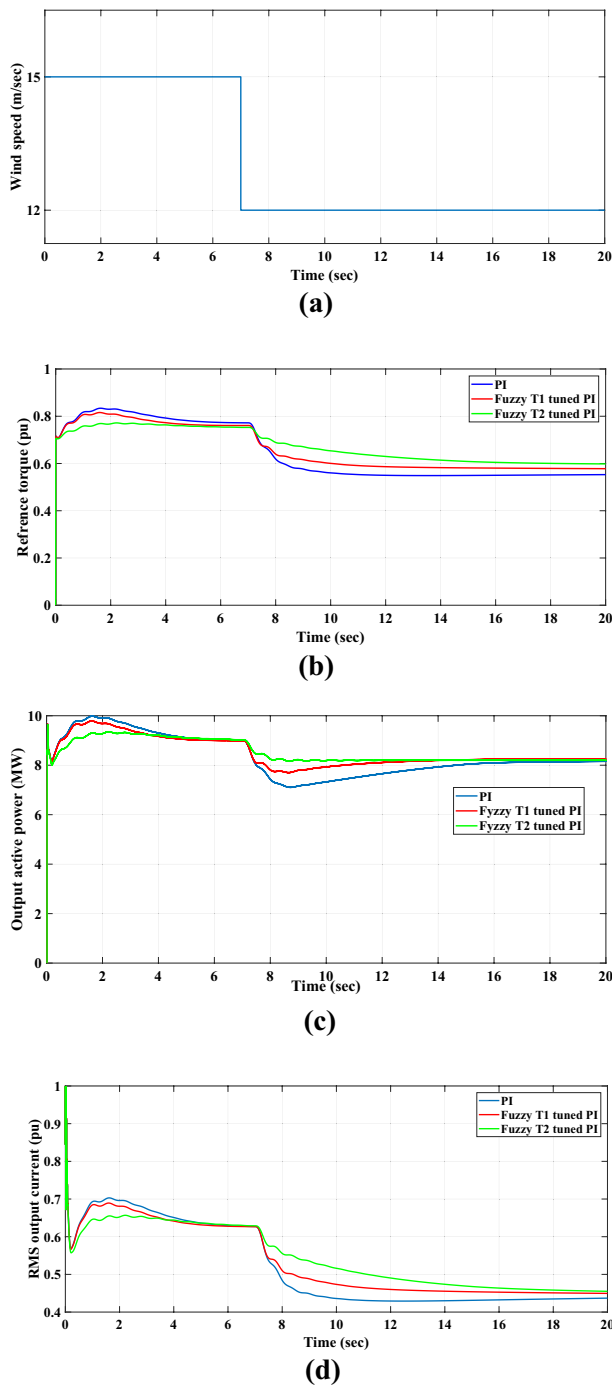**Fig. 9** Configuration of the studied wind farm system

Fig. 10 Step change **a** wind speed, **b** reference torque, **c** output active power, **d** output current

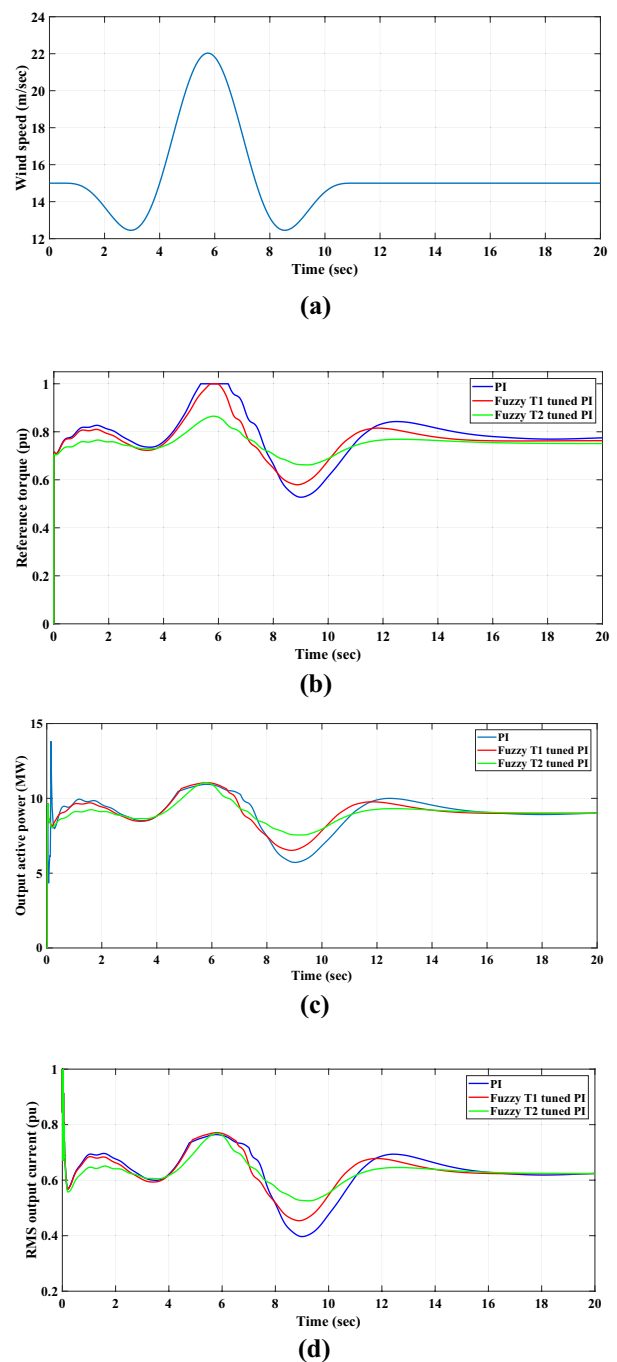**Fig. 11** Extreme change **a** wind speed, **b** reference torque, **c** output active power, **d** output current

equals 13.7 s with type-1 FLC tuned PI and equals 15.5 s with conventional PI. The output power performance is depicted in Fig. 11c. The performance of the RMS output current is shown in Fig. 11d, it is also faster, smoother, and with lower overshoot with interval type-2 FLC tuned PI controller than type-1 fuzzy and PI control. At the beginning of the extreme wind speed, the overshoot of output current equals a little

value of 0.65 pu with interval type-2 FLC. However, the current overshoot equals 0.68 pu and 0.7 pu with type-1 FLC and conventional PI control, respectively. With interval type-2 FLC PI, the current varies more smoothly when the wind speed changes from 12.4 to 22 to 12.4 m/sec than with other controllers. When the wind speed returns to 15 m/sec, the time at which the current reaches steady-state value

with interval type-2 FLC tuned PI equals 12.3 s. However, it equals 13.7 s with type-1 FLC tuned PI and equals 15.5 s with conventional PI.

6.3 Constant wind speed

In this case, the wind speed is fixed at a high value of 18 m/sec as shown in Fig. 12a. The reference torque reaches the steady-state value that equals 0.75 pu with FLC interval type-2 tuned PI controller faster and smoother compared to other controllers as shown in Fig. 12b. The overshoot equals 0.83 pu with type-2 FLC system however it equals 0.94 pu and 0.99 pu with type-1 FLC and conventional PI, respectively. Unlike the fuzzy type-1 and type-2, the PI controller takes a very long time that equals 16.5 s approximately to reach the steady-state. The peak overshoot of output power with FLC interval type-2 PI equals 10.3 MW, however, it equals 10.7 MW with FLC type-1 PI and conventional PI as shown in Fig. 12c. There is a large disturbance in power at the beginning with the conventional PI control. The time taken to reach the steady-state value equals 9 s with conventional PI control and that is very long compared to fuzzy type-1 and type-2. RMS output current performance is illustrated in Fig. 12d, it has lower overshoot with FLC interval type-2 tuned PI controller than type-1 fuzzy and PI control. The overshoot equals 0.72 pu with type-2 FLC system however it equals 0.75 pu with type-1 FLC and conventional PI. The current reaches the steady-state faster with fuzzy type-1 and type-2 than the PI controller. The PI controller takes a very long time that equals 14 s approximately to reach the steady-state however it equals 6 s for type-1 and type-2 FLC approach.

It is obvious from the previously studied cases that the validation of the proposed approach appears in reducing overshoot and the time taken to reach steady state for power, torque, and output current compared to conventional PI control and type-1 FLC tuned PI.

7 Conclusion

In this paper, an approach to regulate the rotor speed of a WT based on DFIG is suggested to adjust the optimum torque that achieves the highest value of power. The suggested control is an interval type-2 FLC tuned PI and compared with other controllers such as type-1 FLC tuned PI and the conventional PI control. The studied model is a wind farm consisting of 6 WTs each of 1.5 MW with a total power of 9 MW. The first studied case is the step change wind speed from 15 m/sec to 12 m/sec at 7 s. At speed of 15 m/sec, the power reaches the steady-state at 2 s with FLC type-2 with no overshoot, however with type-1 FLC and with conventional controller reaches at 3.7 s and 4.7 s,
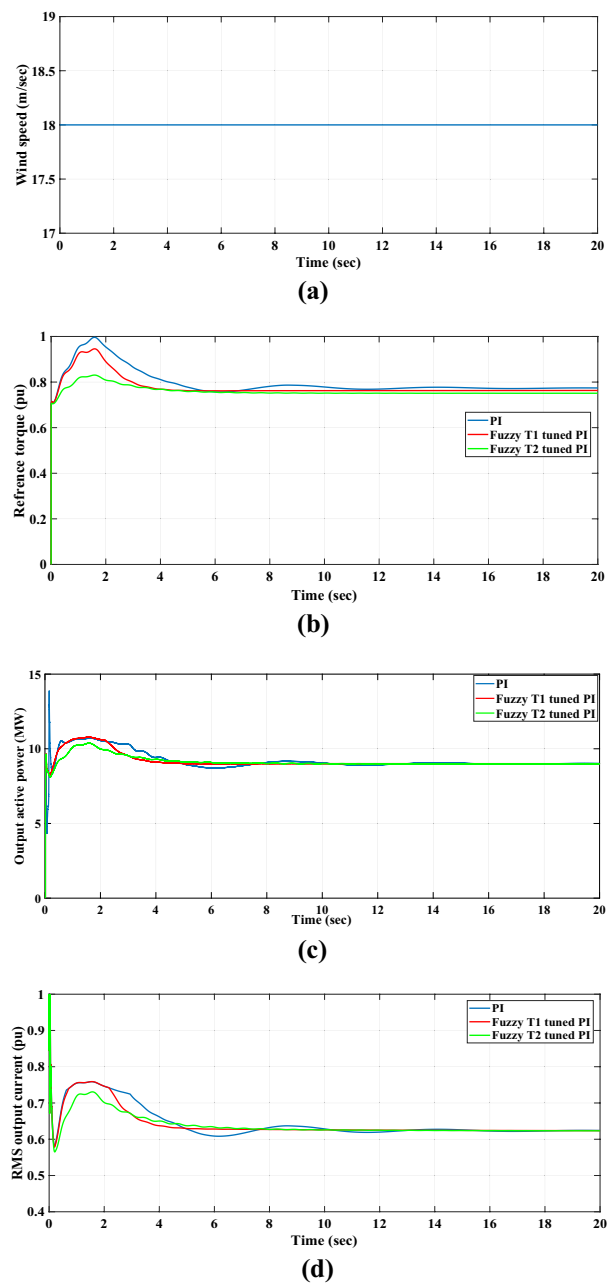

Fig. 12 Constant speed **a** wind speed, **b** reference torque, **c** output active power, **d** output current

and peak overshoot equals 9.78 and 9.98 MW respectively. When the wind changes to 12 m/sec, the power reaches the steady-state at 10 s with type-2 FLC, at 12.8 s with type-1 FLC, and at 18 s with conventional controller. In the second case, the wind speed changes extremely between 15 m/sec, 12.4 m/sec, and 22 m/sec. With a speed of 15 m/sec, the power with type-2 FLC has no overshoot but equals 9.78 and 9.98 MW with FLC type-1 and conventional PI respectively. Then, the power changes more smoothly and faster to reach steady-state with type-2 FLC

tuned PI than other controllers. In the last case, the wind speed is fixed at 18 m/sec. The peak overshoot of output power with type-2 FLC PI equals 10.3 MW, however equals 10.7 MW with FLC type-1 PI and conventional PI. It is obvious from the studied cases that the validation of the proposed approach appears in reducing overshoot and the time taken to reach steady state for power, torque, and output current compared to other control methods.

Data availability Not applicable.

Declarations

Conflict of interest The authors declare no conflict of interest.

Institutional review board statement Not applicable.

Informed consent statement Not applicable.

Research involving human participants and/or animals Not applicable.

References

1. Soomro MA, Memon ZA, Kumar M, Baloch MH (2021) Wind energy integration: dynamic modeling and control of DFIG based on super twisting fractional order terminal sliding mode controller. Energy Rep 7:6031–6043

2. Shabani HR, Kalantar M, Hajizadeh A (2021) Investigation of the closed-loop control system on the DFIG dynamic models in transient stability studies. Int J Electr Power Energy Syst 131:1–21

3. Ayrir W, Ourahou M, El Hassouni B, Haddi A (2020) Direct torque control improvement of a variable speed DFIG based on a fuzzy inference system. Math Comput Simul 167:308–324

4. Abad G, Lopez J, Rodriguez M, Marroyo L, Iwanski G (2011) Doubly fed induction machine: modeling and control for wind energy generation, vol 85. Wiley, Hoboken

5. Sujanarko B, Syafrizal I, Bachri S, Gozali R, Prasetyo S, Hardianto T (2017) Performance improvement of buck-boost converter using fuzzy logic controller. Int J Eng Res Manag (IJERM) 4:22–27

6. Bakouri A, Abbou A, Mahmoudi H, Elyaalaoui K (2014) Direct torque control of a doubly fed induction generator of wind turbine for maximum power extraction. In: 2014 International renewable and sustainable energy conference (IRSEC). IEEE, pp 334–339

7. Ahmed AA, Koh BK, Lee YI (2017) A comparison of finite control set and continuous control set model predictive control schemes for speed control of induction motors. IEEE Trans Industr Inf 14(4):1334–1346

8. Ashouri-Zadeh A, Toulabi M, Bahrami S, Ranjbar AM (2017) Modification of DFIG's active power control loop for speed control enhancement and inertial frequency response. IEEE Trans Sustain Energy 8(4):1772–1782

9. Boubzizi S, Abid H, Chaabane M (2018) Comparative study of three types of controllers for DFIG in wind energy conversion system. Protect Control Mod Power Syst 3(1):1–12

10. Shyu K-K, Shieh H-J, Fu S-S (1998) Model reference adaptive speed control for induction motor drive using neural networks. IEEE Trans Industr Electron 45(1):180–182

11. Masiala M, Vafakhah B, Salmon J, Knight AM (2008) Fuzzy self-tuning speed control of an indirect field-oriented control induction motor drive. IEEE Trans Ind Appl 44(6):1732–1740

12. Liu M, Hu J, Chan KW, Or SW, Ho SL, Xu W, Zhang X (2020) Dual cost function model predictive direct speed control with duty ratio optimization for PMSM drives. IEEE Access 8:126637–126647

13. Sant AV, Rajagopal K (2009) PM synchronous motor speed control using hybrid fuzzy-PI with novel switching functions. IEEE Trans Magn 45(10):4672–4675

14. Benlaloui I, Drid S, Chrifi-Alaoui L, Ouriagli M (2014) Implementation of a new MRAS speed sensorless vector control of induction machine. IEEE Trans Energy Convers 30(2):588–595

15. Raju SK, Pillai G (2015) Design and implementation of type-2 fuzzy logic controller for DFIG-based wind energy systems in distribution networks. IEEE Trans Sustain Energy 7(1):345–353

16. Hemeyine AV, Abbou A, Bakouri A, Mokhlis M, Moustapha E, Ould Mohamed SM (2021) A Robust Interval Type-2 Fuzzy Logic Controller for Variable Speed Wind Turbines Based on a Doubly Fed Induction Generator. Inventions 6(2):1–14

17. Raju SK, Pillai G (2016) Design and real time implementation of type-2 fuzzy vector control for DFIG based wind generators. Renew Energy Int J 88:40–50

18. Rokni Nakhi P, Ahmadi Kamarposhti M (2020) Multi objective design of type II fuzzy based power system stabilizer for power system with wind farm turbine considering uncertainty. Int Trans Electr Energy Syst 30(4):1–20

19. Villanueva I, Ponce P, Molina A (2015) Interval type 2 fuzzy logic controller for rotor voltage of a doubly-fed induction generator and pitch angle of wind turbine blades. IFAC-PapersOnLine 48(3):2195–2202

20. Hosseini S, Manthouri M (2022) Type 2 adaptive fuzzy control approach applied to variable speed DFIG based wind turbines with MPPT algorithm. Iranian J Fuzzy Syst 19(1):31–45

21. Ferhat N, Aounallah T, Essounbouli N, Bouchafaa F, Hamzaoui A (2021) Adaptive interval type 2 fuzzy fractional order sliding mode control for permanent magnet synchronous generators. In: 2021 9th international conference on systems and control (ICSC). IEEE, pp 139–144

22. Gencer A (2019) Analysis and control of low-voltage ride-through capability improvement for PMSG based on an NPC converter using an interval type-2 fuzzy logic system. Elektronika ir Elektrotechnika 25(3):63–70

23. Sahri Y, Tamalouzt S, Lalouni Belaid S, Bacha S, Ullah N, Ahamdi AAA, Alzaed AN (2021) Advanced fuzzy 12 DTC control of doubly fed Induction generator for optimal power extraction in wind turbine system under random wind conditions. Sustainability 13(21):1–23

24. Wiam A, Ali H (2019) Direct torque control-based power factor control of a DFIG. Energy Procedia 162:296–305

25. Deng Z, Cao Y, Lou Q, Choi K-S, Wang S (2022) Monotonic relation-constrained Takagi-Sugeno-Kang fuzzy system. Inf Sci Int J 582:243–257

26. Giannakis A, Karlis A, Karnavas YL (2018) A combined control strategy of a DFIG based on a sensorless power control through modified phase-locked loop and fuzzy logic controllers. Renew Energy Int J 121:489–501

27. Civelek Z (2020) Optimization of fuzzy logic (Takagi-Sugeno) blade pitch angle controller in wind turbines by genetic algorithm. Eng Sci Technol Int J 23(1):1–9

28. Karnik N, Mendel J (1998) An introduction to type-2 fuzzy logic systems, technical report. IEEE Trans Fuzzy Syst. https://doi.org/10.1109/91.811231

29. Mittal K, Jain A, Vaisla KS, Castillo O, Kacprzyk J (2020) A comprehensive review on type 2 fuzzy logic applications: past, present and future. Eng Appl Artif Intell 95:1–12

30. Hagras H, Wagner C (2012) Towards the wide spread use of type-2 fuzzy logic systems in real world applications. IEEE Comput Intell Mag 7(3):14–24

31. Li J, Yang L, Fu X, Chao F, Qu Y (2018) Interval type-2 tsk+ fuzzy inference system. In: 2018 IEEE International Conference on Fuzzy Systems (FUZZ-IEEE). IEEE, pp 1–8

32. Mendel JM, Hagras H, Bustince H, Herrera F (2015) Comments on "Interval type-2 fuzzy sets are generalization of interval-valued fuzzy sets: towards a wide view on their relationship." IEEE Trans Fuzzy Syst 24(1):249–250

33. Naik KA, Gupta CP, Fernandez E (2020) Design and implementation of interval type-2 fuzzy logic-PI based adaptive controller for DFIG based wind energy system. Int J Electr Power Energy Syst 115:1–16

34. Djamila C, Yahia M (2020) Direct torque control strategies of induction machine: comparative studies. In: Direct torque control strategies of electrical machines. IntechOpen, pp 17–38

35. Goyal S, Gaur M, Bhandari S (2013) Power regulation of a wind turbine using adaptive fuzzy-PID pitch angle controller. Int J Recent Technol Eng 2(3):128–132